



Short communication

A CO-tolerant PtRu catalyst supported on thiol-functionalized carbon nanotubes for the methanol oxidation reaction



Lin Guo, Sigu Chen*, Li Li, Zidong Wei*

The State Key Laboratory of Power Transmission Equipment & System Security and New Technology, College of Chemistry and Chemical Engineering, Chongqing University, Chongqing 400044, China

HIGHLIGHTS

- The PtRu/SH-CNTs catalyst has shown higher MOR activity than the PtRu/COOH-CNTs catalyst.
- The weakened CO adsorption diminishes the poisoning of the PtRu/SH-CNTs catalyst.
- The strong interaction between Pt and SH-CNTs has weakened the CO adsorption on Pt atoms.

ARTICLE INFO

Article history:

Received 4 June 2013

Received in revised form

19 August 2013

Accepted 22 August 2013

Available online 3 September 2013

Keywords:

Direct methanol fuel cell

Carbon monoxide tolerance

Platinum ruthenium alloy

Thiol-functionalized carbon nanotubes

Catalytic activity

ABSTRACT

PtRu nanoparticles (NPs) with enhanced methanol oxidation are prepared by a simple chemical reduction method using the thiol-functionalized carbon nanotubes (SH-CNTs) as support. Electrochemical measurements confirmed that the higher methanol oxidation is due to the excellent CO tolerance of PtRu NPs. From the comparison with the PtRu/COOH-CNTs catalyst, the experiment results demonstrate that excellent CO tolerance is originated from the strong interaction between Pt atoms and the –SH groups, which weakens CO adsorption and leads a higher methanol oxidation activity.

© 2013 Published by Elsevier B.V.

1. Introduction

Direct methanol fuel cells (DMFCs) are promising power sources for portable electronics because they operate at room temperature, use liquid methanol as the fuel, and eliminate the expensive setup of hydrogen reformers and the hydrogen storage problem [1–3]. However, the two key barriers to their commercialization are their sluggish anode kinetics and noble Pt catalyst poisoning by intermediate CO generated by methanol oxidation reaction (MOR) [4–6]. Efforts to explore CO-tolerant catalysts have been ongoing for several decades so that this efficient technology can be used in real applications [7–10]. Until now, the most efficient approach to protect Pt NPs from CO poisoning is the introduction of a secondary metal M into the Pt [11–14]. Among different bimetallic catalysts,

PtRu has attracted the most attention due to its strong CO tolerance and MOR enhancement, which can be explained by the “bifunctional mechanism” [15], “electronic effect” [16], or a combination of the two [17,18].

In addition to the modification of the Pt catalyst by incorporating secondary metals, the development of an appropriate support is another way to improve the performance of Pt-based catalysts [19–23]. Over the last decades, different modified carbon materials have been tested for this purpose [24–26]. Although high specific area, good conductivity and excellent electrochemical durability of the carbon supports are considered to be the extremely important features for improving the catalytic activity of the Pt-based catalysts, the potential of the electronic interaction between the carbon support and the Pt-based catalysts in promoting the catalytic activity should not be ignored. To date, there is little research to specially investigate the effect of the electronic interaction between the carbon supports and the Pt-based catalysts on the MOR activity. In our earlier study on the oxygen reduction reaction, we used thiol-functionalized carbon nanotubes (SH-CNTs)

* Corresponding authors. Tel.: +86 23 65105161 (lab.), +86 23 65112134; fax: +86 23 65102531.

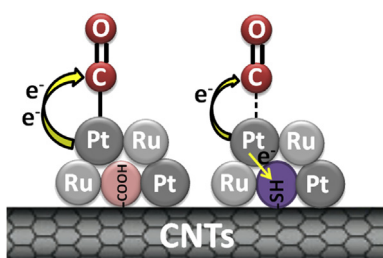
E-mail addresses: csg810519@126.com (S. Chen), zdwei@cqu.edu.cn (Z. Wei).

as a catalyst support, and the dispersion and durability of Pt NPs were markedly improved due to the strong interaction between Pt and SH-CNTs [27]. Inspired by the effect of SH-CNTs on Pt, we present here a CO-tolerant PtRu anode catalyst using SH-CNTs support toward methanol oxidation. Generally, CO is adsorbed on Pt due to coupling of the CO 5σ orbital to Pt [28]. The $\sigma-\pi$ bond is strengthened by the back-donation of electrons from Pt to the $2\pi^*$ orbital of the CO molecule. Therefore, any measure that can inhibit the electron transfer from the Pt $d\pi$ to CO $2\pi^*$ orbital could weaken the $\sigma-\pi$ bond and CO adsorption strength on Pt; accordingly, such a measure is conducive to the removal of CO from the Pt surface, as shown in **Scheme 1**. The results also illustrate that the strong Pt–SH interaction can significantly inhibit electron transfer from Pt, thus lowering the CO adsorption energy on PtRu NPs and enhancing MOR activity. The performance of the prepared PtRu/SH-CNT catalysts for the MOR is monitored and compared with that of a PtRu/COOH-CNTs catalyst.

2. Experimental

The SH-CNT sample was prepared by successive purification, carboxylation, reduction, bromination and thiolation [27]. The deposition of PtRu nanoparticles (NPs) (1:1 atomic ratio, 20 wt%) on the SH-CNTs was achieved via a chemical reduction process. The details were as follows: SH-CNTs, H_2PtCl_6 and $RuCl_3$ were mixed with a solution of THF/H_2O (1:1), exposed to ultrasonic treatment for 30 min and then mechanically stirred for 24 h. PtRu NPs were formed and anchored on the support after a solution of $NaBH_4$ and Na_2CO_3 was added at room temperature and allowed to react for 1 h. The resulting samples were filtered, washed with distilled water, and dried at 60 °C. The products were called the PtRu/SH-CNTs catalyst. For comparison, the deposition of PtRu NPs on COOH-CNTs was conducted according to the same procedure. The products were called PtRu/COOH-CNTs.

All potentials are given relative to the reversible hydrogen electrode (RHE). To prepare the PtRu/CNTs working electrode, the electrocatalyst was dispersed in ethanol and ultrasonicated for 10 min to form a uniform catalyst ink. The obtained 10 μL slurry was placed on the surface of a glassy carbon electrode with a 5 mm diameter. After drying, a drop of 0.5 wt% Nafion solution was applied to the surface of the catalyst layer to form a thin protective film. The electrolyte was purged with high-purity nitrogen for at least 15 min prior to measurements to remove dissolved oxygen, unless otherwise stated. The methanol oxidation experiment was conducted in 0.5 M H_2SO_4 + 1 M CH_3OH solution with a scan rate 10 $mV s^{-1}$. For the CO-stripping measurements, the catalyst surface was first saturated with CO by bubbling CO through a 0.5 M H_2SO_4 solution while the working electrode was held at 0 V for 15 min. The remaining CO was purged by flowing N_2 for 30 min before the measurements were taken.



Scheme 1. The $\sigma-\pi$ bond of CO–Pt is weakened by inhibition of the electron transfer with the introduction of –SH to CNTs.

3. Results and discussion

Raman spectroscopy was used to examine the SH-CNTs. As shown in **Fig. 1**, there is a new peak at 689 cm^{-1} on SH-CNTs compared to COOH-CNTs, which is attributed to the C–S vibration and also demonstrates the successful introduction of –SH groups on CNTs. The morphology and structural properties of PtRu NPs supported on SH-CNTs and COOH-CNTs were determined by TEM and XRD, as discussed below. **Fig. 2** presents TEM images of the PtRu/SH-CNTs (**Fig. 2a**) and PtRu/COOH-CNTs catalysts (**Fig. 2c**). The TEM images reveal that the PtRu NPs are highly dispersed on SH-CNTs and COOH-CNTs. The average particle sizes of the PtRu/SH-CNTs and PtRu/COOH-CNTs catalysts are 3.5 nm (**Fig. 2b**) and 4 nm (**Fig. 2d**), respectively, indicating that the PtRu/SH-CNTs and PtRu/COOH-CNTs have similar morphologies and particle size distributions.

To further verify the structure of these catalysts, XRD patterns of the PtRu/SH-CNTs and PtRu/COOH-CNTs catalysts are presented in **Fig. 2e**. The XRD patterns show three characteristic peaks corresponding to the (111), (200) and (220) planes of Pt crystal with the face-centered-cubic (fcc) structure. The diffraction peaks of the two catalysts are very similar and are shifted to a higher 2θ value compared with the peak position of pure Pt (JCPDS card 04-0802), indicating that Ru atoms entered into the Pt lattice, and the PtRu alloy was already formed. The Pt (220) diffraction peak, which was not disturbed by the diffraction peak of the carbon support, was used to calculate the structural data [29,30]. The lattice parameter of the PtRu particles and the alloying extent of Pt and Ru for the PtRu/SH-CNTs catalyst are 0.38823 nm and 27.4%, respectively. The corresponding data for the PtRu/COOH-CNTs catalyst are 0.38818 nm and 27.7%, respectively. The atomic ratio of all the elements in the PtRu/SH-CNT and PtRu/COOH-CNT catalysts obtained from the X-ray photoelectron spectroscopy (XPS) are 88.95:5.01:1.19:4.27:0.58 (C:O:Pt:Ru:S) and 89.48:4.62:1.39:4.51 (C:O:Pt:Ru), respectively. It can be clearly observed from the above data that the two catalysts have an identical alloying extent and the similar surface composition.

To examine the catalytic activity of the PtRu/SH-CNT and PtRu/COOH-CNT catalysts in the MOR, linear sweep voltammograms (LSV) of the two catalysts were recorded in N_2 -saturated 1 M CH_3OH + 0.5 M H_2SO_4 solution at a scan rate of 10 $mV s^{-1}$. As shown in **Fig. 3a**, the onset potential of the MOR on the PtRu/SH-CNTs catalyst (~ 0.37 V) is more negative than it is on the PtRu/COOH-CNTs catalyst (~ 0.41 V). The peak current density of the former (9.71 mA cm^{-2}) is approximately 1.7 times higher than that of the latter (5.72 mA cm^{-2}), indicating that PtRu/SH-CNTs have enhanced catalytic activity for the MOR. Chronoamperometry (CA) was employed to investigate the electrochemical activity and stability of

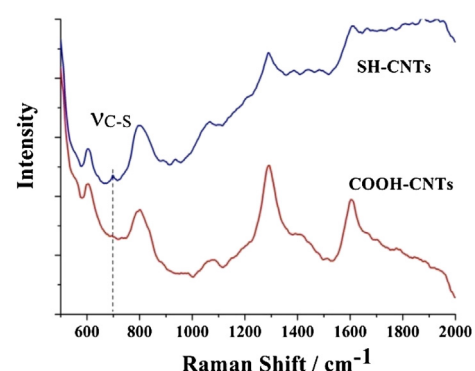


Fig. 1. Raman spectra of the SH-CNTs and COOH-CNTs.

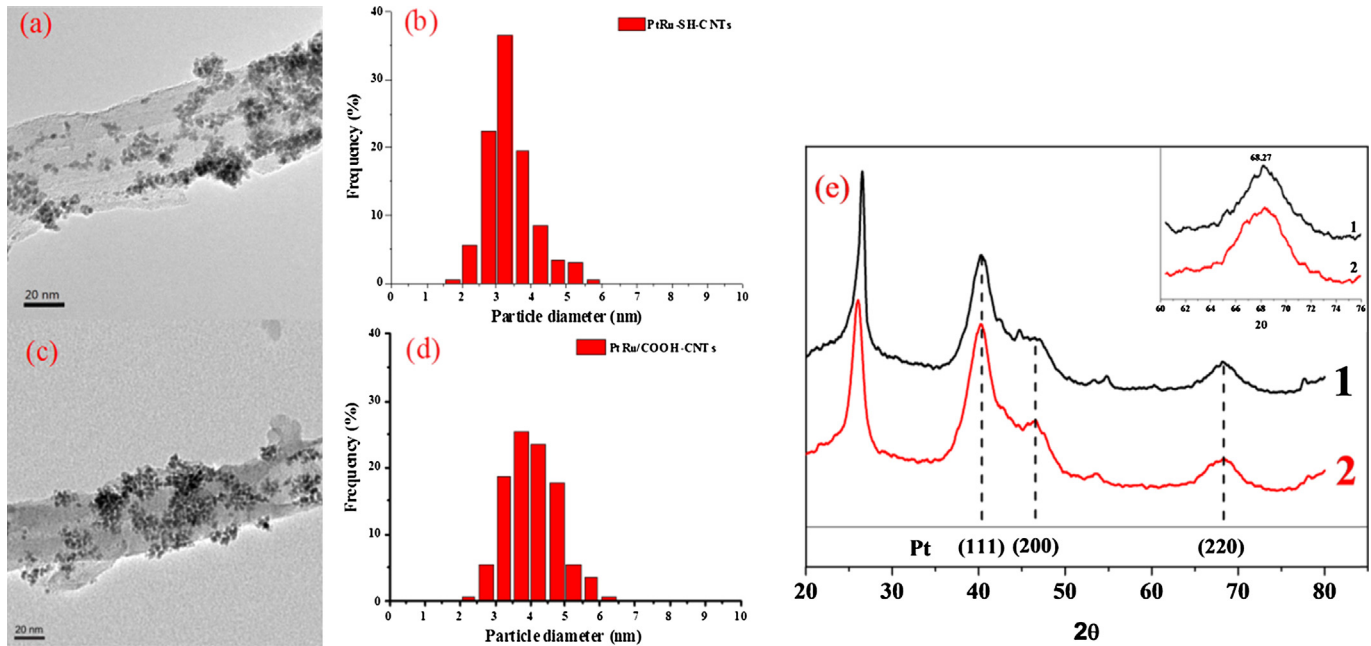


Fig. 2. TEM images of PtRu NPs deposited on the SH-CNTs (a) and COOH-CNTs (c) and their NP size distributions, (b) and (d). (e) XRD patterns of the PtRu/SH-CNTs (1) and PtRu/COOH-CNTs (2).

the different catalysts, as shown in Fig. 3b. The PtRu/SH-CNTs catalyst for the MOR showed higher current density and slower attenuation than the PtRu/COOH-CNTs catalyst.

In order to investigate the enhanced methanol oxidation on PtRu/SH-CNTs catalyst, CO stripping voltammograms were recorded in N_2 -saturated 0.5 M H_2SO_4 solution at a scan rate of

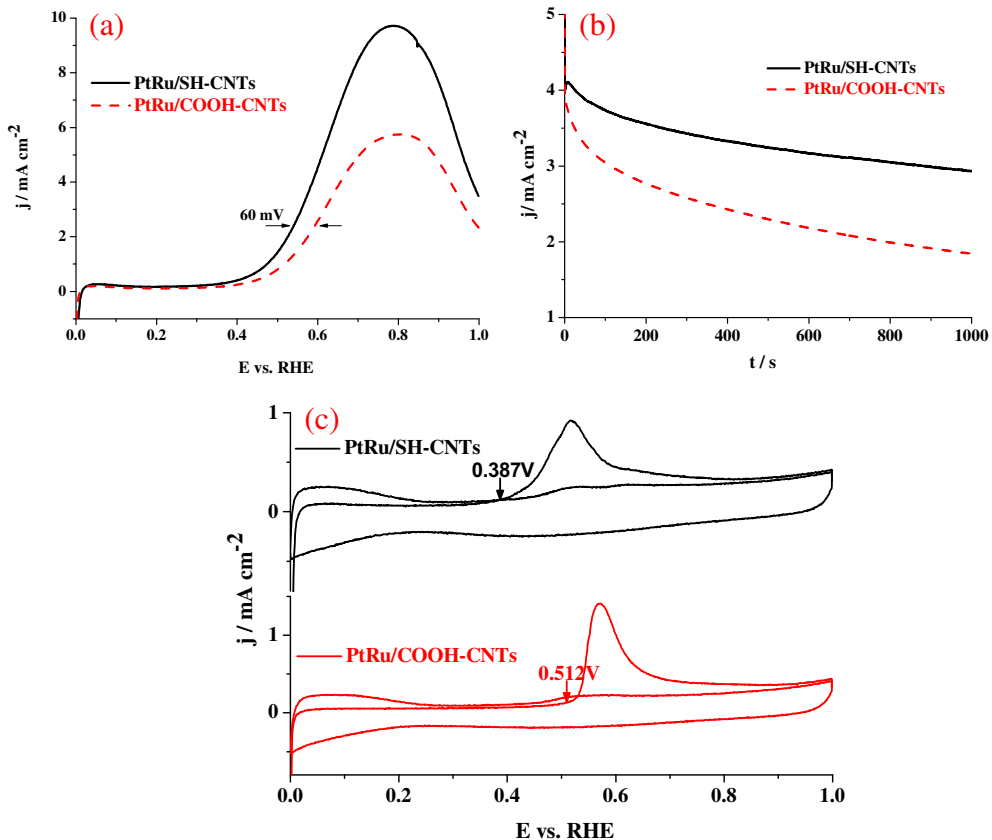


Fig. 3. (a) Linear sweep voltammograms of the PtRu/SH-CNT and PtRu/COOH-CNT catalysts in N_2 -saturated 1 M $CH_3OH + 0.5$ M H_2SO_4 solution at a scan rate of 10 mV s^{-1} . (b) Chronoamperometry of the PtRu/SH-CNT and PtRu/COOH-CNT catalysts at potential of 0.6 V in 1 M $CH_3OH + 0.5$ M H_2SO_4 solution. (c) CO stripping cyclic voltammograms of the PtRu/SH-CNT and PtRu/COOH-CNT catalysts in N_2 -saturated 0.5 M H_2SO_4 solution at a scan rate of 10 mV s^{-1} .

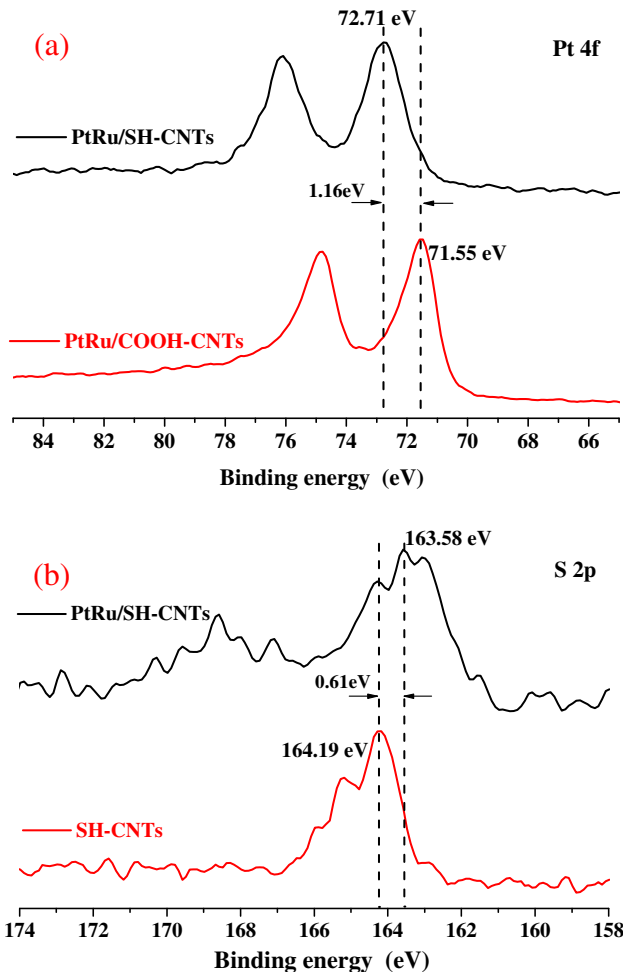


Fig. 4. (a) Pt 4f XPS spectra of the PtRu/SH-CNT and PtRu/COOH-CNT catalysts, (b) S 2p XPS spectra of the PtRu/SH-CNT catalyst and SH-CNTs.

10 mV s⁻¹. Fig. 3c shows that the CV for CO adsorption on the PtRu surfaces peaks in a potential range from 0 to 0.3 V, indicating that the hydrogen adsorption/desorption is absolutely suppressed. The CO anodic oxidation on the PtRu/SH-CNTs catalyst surface (0.387 V) starts much earlier than on the PtRu/COOH-CNTs catalyst (0.512 V), clearly confirming that the PtRu/SH-CNTs catalyst can facilitate the electrooxidation of CO. To further understand the CO oxidation ability of the two catalysts, the electrochemically active surface area (ECSA) was calculated by measuring the Coulombic charge for CO adsorption. The specific values of the ECSA based on the Pt mass for the PtRu/SH-CNTs and PtRu/COOH-CNTs catalysts are estimated to be 68.5 and 71.2 m² g⁻¹, respectively. Thus, the calculated specific surface activities for the PtRu/SH-CNTs and PtRu/COOH-CNTs catalysts are 2.14 and 1.21 A m⁻², respectively. In combination with the LSV and CA measurements, the results suggest that the enhanced electrooxidation activity of CO diminishes the poisoning of the PtRu/SH-CNTs catalyst and leads to a higher methanol oxidation activity.

Considering that the two catalysts, PtRu/SH-CNTs and PtRu/COOH-CNTs, have the identical alloying extent and the similar particle size, the significant enhancement of the PtRu/SH-CNTs on activity should be mainly due to the special interaction between PtRu NPs and SH-CNTs resulting from the existence of –SH groups. To further elucidate the role of the –SH group, X-ray photoelectron spectroscopy (XPS) of Pt 4f in the PtRu/SH-CNTs and PtRu/COOH-

CNTs catalysts was investigated. The results (Fig. 4a) show that the Pt 4f_{7/2} peak in the PtRu/SH-CNTs shifts to a higher binding energy (72.71 eV) compared with that in the PtRu/COOH-CNTs (71.55 eV), indicating that electron transfer from PtRu/SH-CNTs becomes more difficult than electron transfer from PtRu/COOH-CNTs. Therefore, the σ–π bond of Pt–CO, which depends on the electron back-donation from Pt, is not as strong in the case of the PtRu/SH-CNTs as it is in the PtRu/COOH-CNTs. In other words, CO adsorption on Pt in the PtRu/SH-CNTs is not as strong as that in the PtRu/COOH-CNTs. Accordingly, CO adsorption on Pt in the PtRu/SH-CNTs is more easily removed than it is in the PtRu/COOH-CNTs. The above-mentioned phenomena can be attributed to the strong interaction between Pt and SH-CNTs, which leads to electron transfer from Pt to the SH-CNTs. This assertion is supported by the shift of the S 2p peak (Fig. 4b) of the PtRu/SH-CNTs to lower binding energy compared with that of the SH-CNTs. This shift indicates that there are more electrons in the S 2p orbital in PtRu/SH-CNTs than in SH-CNTs. The strong interaction between Pt and SH-CNTs weakens the interaction between Pt atoms and CO and facilitates the removal of CO on the PtRu NP surface.

4. Conclusion

In summary, we successfully prepared a CO-tolerant PtRu/SH-CNTs catalyst with an enhanced MOR activity using SH-CNTs as a catalyst support. A comparative study on the electrocatalytic activity towards methanol oxidation shows that PtRu/SH-CNTs are much more active. The enhanced catalytic activity is attributed to the strong Pt–SH interaction that weakens the σ–π bond between CO and Pt. This work suggests that the PtRu/SH-CNTs catalyst could be promising anode electrocatalysts for direct methanol fuel cells with high activity and CO poisoning resistance.

Acknowledgments

This work was financially supported by the China National 973 Program (2012CB215500 and 2012CB720300), the NSFC (Grants 20936008, 51072239, 21276291 and 21176327).

References

- [1] M. Winter, R.J. Brodd, Chem. Rev. 104 (2004) 4245–4270.
- [2] Y.L. Hsin, K.C. Hwang, C.T. Yeh, J. Am. Chem. Soc. 129 (2007) 9999–10010.
- [3] A.A. Dameron, T.S. Olson, S.T. Christensen, J.E. Leisch, K.E. Hurst, S. Pylypenko, J.B. Bult, D.S. Ginley, R.P. O’Hayre, H.N. Dinh, T. Gennett, ACS Catal. 1 (2011) 1307–1315.
- [4] S. Park, A. Wieckowski, M.J. Weaver, J. Am. Chem. Soc. 125 (2003) 2282–2290.
- [5] J.Y. Xi, J.S. Wang, L.H. Yu, X.P. Qiu, L.Q. Chen, Chem. Commun. 16 (2007) 1656–1658.
- [6] L. Cao, F. Scheiba, C. Roth, F. Schweiger, C. Cremers, U. Stimming, H. Fuess, L.Q. Chen, W.T. Zhu, X.P. Qiu, Angew. Chem. Int. Ed. 45 (2006) 5315–5319.
- [7] Z.D. Wei, L.L. Li, Y.H. Luo, C. Yan, C.X. Sun, G.Z. Yin, P.K. Shen, J. Phys. Chem. B 110 (2006) 26055–26061.
- [8] Z.F. Liu, J.E. Hu, Q. Wang, K. Gaskell, A.I. Frenkel, G.S. Jackson, B. Eichhorn, J. Am. Chem. Soc. 131 (2009) 6924–6925.
- [9] Y.Q. Wang, Z.D. Wei, B. Gao, X.Q. Qi, L. Li, Q. Zhang, M.R. Xia, J. Power Sources 196 (2011) 1132–1135.
- [10] Z.M. Cui, S.P. Jiang, C.M. Li, Chem. Commun. 47 (2011) 8418–8420.
- [11] Y. Chen, Y.W. Tang, C.P. Liu, W. Xing, T.H. Lu, J. Power Sources 161 (2006) 470–473.
- [12] H.Z. Yang, J. Zhang, K. Sun, S.Z. Zou, J.Y. Fang, Angew. Chem. Int. Ed. 49 (2010) 6848–6851.
- [13] C. Dupont, Y. Jugnet, D. Loffreda, J. Am. Chem. Soc. 128 (2006) 9129–9136.
- [14] Y. Liu, D. Li, V.R. Stamenkovic, S. Soled, J.D. Henao, S. Sun, ACS Catal. 1 (2011) 1719–1723.
- [15] M. Watanabe, S. Motoos, J. Electroanal. Chem. 60 (1975) 267–273.
- [16] Y.Y. Tong, H.S. Kim, P.K. Babu, P. Waszczuk, A. Wieckowski, E. Oldfield, J. Am. Chem. Soc. 124 (2002) 468–473.
- [17] C. Lu, C. Rice, R.I. Masel, P.K. Babu, P. Waszczuk, H.S. Kim, E. Oldfield, A. Wieckowski, J. Phys. Chem. B 106 (2002) 9581–9589.
- [18] C. Roth, N. Benker, T. Buhrmester, M. Masurek, M. Loster, H. Fuess, D.C. Koningsberger, D.E. Ramaker, J. Am. Chem. Soc. 127 (2005) 14607–14615.

- [19] B.H. Wu, D. Hu, Y.J. Kuang, B. Liu, X.H. Zhang, J.H. Chen, *Angew. Chem. Int. Ed.* 48 (2009) 4751–4754.
- [20] J. Oh, T. Kondo, D. Hatake, Y. Iwasaki, Y. Honma, Y. Suda, D. Sekiba, H. Kudo, J. Nakamura, *J. Phys. Chem. Lett.* 1 (2010) 463–466.
- [21] C.M. Zhou, H.J. Wang, F. Peng, J.H. Liang, H. Yu, J. Yang, *Langmuir* 25 (2009) 7711–7717.
- [22] G.H. Lee, J.H. Shim, H.Y. Kang, K.M. Nam, H.J. Song, J.T. Park, *Chem. Commun.* 33 (2009) 5036–5038.
- [23] B.H. Wu, D. Hu, Y.J. Kuang, Y.M. Yu, X.H. Zhang, J.H. Chen, *Chem. Commun.* 47 (2011) 5253–5255.
- [24] H.Y. Lee, W. Vogel, P.P. Chu, *Langmuir* 27 (2011) 14654–14661.
- [25] Y.T. Kim, H. Lee, H.J. Kim, T.H. Lim, *Chem. Commun.* 46 (2010) 2085–2087.
- [26] Y.T. Kim, T. Mitani, *J. Catal.* 238 (2006) 394–401.
- [27] S.G. Chen, Z.D. Wei, L. Guo, W. Ding, L.C. Dong, P.K. Shen, X.Q. Qi, L. Li, *Chem. Commun.* 47 (2011) 10984–10986.
- [28] D.Y. Wang, H.L. Chou, Y.C. Lin, F.J. Lai, C.H. Chen, J.F. Lee, B.J. Hwang, C.C. Chen, *J. Am. Chem. Soc.* 134 (2012) 10011–10020.
- [29] A. Velazquez, F. Centellas, J.A. Garrido, C. Arias, R.M. Rodriguez, E. Brillas, P.L. Cabot, *J. Phys. Chem. C* 114 (2010) 4399–4407.
- [30] Y.L. Page, C. Bock, J.R. Rodgers, *J. Alloys Compd.* 422 (2006) 164–172.